BULLETIN OF THE CHEMICAL SOCIETY OF JAPAN, VOL. 46, 3665—3671 (1973)

Kinetics of Hydrogen Electrode Reaction on Mercury. I. Theoretical Part. Non-steady State Analysis for the Electrochemical Mechanism

Akiko KATAYAMA and Hideaki KITA

Research Institute for Catalysis, Hokkaido University, Sapporo 060

(Received July 2, 1973)

Potentiostatic and potentiodynamic transients are theoretically analysed on the basis of the electrochemical mechanism for the hydrogen electrode reaction. The interface was assumed to consist of the metal surface, the plane on which the adsorbed intermediate of $H_2^+(a)$ stays, and the diffuse double layer. The repulsive force between the intermediates was introduced by proportional approximation. From the results the depolarization observed in Tafel plots is understood as a non-steady state phenomenon, and observation by the potential-sweep method offers information on both the features of the adsorbed intermediate and the kinetics of the step preceding the rate-determining step.

In 1936 Horiuti and Okamoto found[1] that experimental values on the separation factor of the hydrogen evolution reaction serve to classify electrode metals into two groups. A dual mechanism was proposed[2,3] for the hydrogen electrode reaction (H.E.R.) on these groups of metals, *i.e.*, catalytic mechanism on Pt (at high overvoltages), Ni, Au, Cu, and Pb (in alkaline solution), and electrochemical mechanism on Hg, Pb (in acidic solution), Sn, and Pt (at low overvoltages). One of the present authors (H.K.)[4] surveyed data of H.E.R. on various metals reported for the last two decades and examined the relationship between the catalytic activity of electrodes and the heat of adsorption of hydrogen or the work function. A grouping of metals similar to Horiuti's was found, transition metals including IB metal (Cu, Ag, Au) being denoted by "d-metal" and those after IIB in the periodic table by "sp-metals". He showed that the difference between d- and sp-metals can be explained by the dual mechanism, *i.e.*, the catalytic mechanism on d-metals and the electrochemical mechanism on sp-metals.

The electrochemical mechanism consists of the following consecutive steps:

$$2H^+ + e^- \rightleftarrows H_2^+(a) \quad \text{(I)}$$

$$H_2^+(a) + e^- \rightarrow H_2, \quad \text{(II)}$$

1) J. Horiuti and G. Okamoto, *Sci. Pap., I.P.C.R.*, (Tokyo), **28**, 23, (1936).

2) G. Okamoto, J. Horiuti, and K. Hirota, *ibid.*, **29**, 223 (1936).

3) J. Horiuti, T. Keii, and K. Hirota, *J. Res. Inst. Catal., Hokkaido Univ.*, **2**, 1 (1951).

4) H. Kita, *J. Electrochem. Soc.*, **113**, 1095 (1966).

where (II) is the rate-determining step and $H_2^+(a)$ is a hydrogen-molecule ion adsorbed on the electrode. However, the mechanism most frequently quoted, especially for Hg,[5] is the slow discharge mechanism, in which the rate-determining step is the formation of an adsorbed hydrogen atom, H(a); $H^+ + e^- \rightarrow H(a)$. This mechanism seems to be widely accepted because it provides the simplest way for an explanation of the kinetics observed. However, for Hg many experimental results which cannot be explained easily by means of the slow discharge mechanism have been obtained, *e.g.*, prolonged evolution of hydrogen gas after cessation of a cathodic polarization,[6,7] abnormal shift of a half-wave potential $E_{1/2}$ under various conditions,[6,8] and large transfer coefficient (>0.5) observed by the faradaic rectification method.[9] The prolonged evolution of hydrogen gas indicates that the rate-determining step is preceded by a fast step which produces an intermediate. According to the simple discharge mechanism, $E_{1/2}$ is not expected to shift with the pH of the solution, but this is not the case.[8] The effect of the column height of dropping mercury electrode on $E_{1/2}$ differs from that expected from the slow discharge mechanism. The symmetrical polarogram predicted from the slow discharge mechanism was not also observed under various conditions.[6] Barker found a larger value for a transfer coefficient by the sophisticated method of the faradaic rectification and attributed it to H_2^+ formation.[9]

Horiuti *et al.* who proposed the electrochemical mechanism, predicted the change in the Tafel slope from 40 to 120 mV on Hg with increase of a cathodic polarization. Experimental results, however, show the depolarization at low overvoltages; the observed current density is much higher than that extrapolated from the linear part of Tafel plots observed at high overvoltages. A possible explanation for the depolarization is to consider it a non-steady state phenomenon. As seen from an extremely small exchange current density of $10^{-12} \sim 10^{-13}$ A/cm^2 on Hg,[4] it may take a considerably long time for H.E.R. to attain a steady state, especially at low overvoltages. The reaction will then appear to be in a steady state on the time scale of usual observation though in fact it is not.

In the present work we attempt to interpret H.E.R. on Hg in a non-steady state and its transient process to attainment of steady state, assuming the electrochemical mechanism. A theoretical analysis is described.

Formulation

In the case of the electrochemical mechanism, the non-steady state is expressed by

$$Q\mathrm{d}\theta/\mathrm{d}t = i_1 - i_2 \neq 0, \tag{1}$$

where Q represents a monolayer quantity of $H_2^+(a)$ in electricity, θ the coverage of $H_2^+(a)$, and i_1 and i_2 net currents of steps (I) and (II), respectively. Non-steady state analysis is to solve the above equation for i_1 and i_2, and hence for the total current i,

$$i = i_1 + i_2, \tag{2}$$

as a function of time.

Rate expression. We first treat the rate expressions for i_1 and i_2. Horiuti developed a generalized theory for a reaction rate,[10,11] which gives precise rate formulae even for the heterogeneous reaction. On the basis of a crystal lattice plane model, forward and backward velocities of an elementary step are expressed in current densities by

$$i_+ = F(kT/h)N^{\neq}\theta^{\neq}(0)\exp\{-(\varepsilon^{\neq}-\mu^{\mathrm{I}})/RT\} \tag{3}$$

and

$$i_- = F(kT/h)N^{\neq}\theta^{\neq}(0)\exp\{-(\varepsilon^{\mathrm{I}}-\mu^{\mathrm{F}})/RT\}, \tag{4}$$

where the number of electrons concerned is put to unity. In Eqs. (3) and (4), $\neq$ is a critical system, $N^{\neq}$ the total number of sites for $\neq(\sigma^{\neq})$ per unit area, $\varepsilon^{\neq}$ reversible work required for a critical system to be brought from a standard state to a vacant $\sigma^{\neq}$, $\theta^{\neq}(0)$ the probability of $\sigma^{\neq}$ being vacant, μ^{I} and μ^{F} chemical potentials of the initial and final systems of a step, respectively. F, k, T, and h have their usual meanings.

In order to develop the rate expressions further, we introduce the following four relations.

(a). When the adsorption site of a critical system is the same as that of $H_2^+(a)$, we have

$$\theta^{\neq}(0) = 1 - \theta, \tag{5}$$

where θ represents the coverage of $H_2^+(a)$.

(b). Another fundamental relation is used:[10]

$$\theta/(1-\theta) = \exp\{[\mu(H_2^+) - \varepsilon(H_2^+)]/RT\}, \tag{6}$$

where $\varepsilon(H_2^+)$ is defined as reversible work required for $H_2^+(a)$ to be brought from a standard state to a vacant $\sigma^{\neq}$ (for the sake of simplicity abbreviated to ε). The functions μ^{I}, μ^{F}, and $\varepsilon^{\neq}$ for steps (I) and (II) are summarized in Table 1, where $\mu(H^+)$, $\mu(e^-)$, and $\mu(H_2)$ are chemical potentials of proton, metal electron, and hydrogen gas, respectively.

Table 1. μ^{I} and μ^{F} for steps (I) and (II)

	Step (I)		Step (II)	
μ^{I}	$2\mu(H^+)+\mu(e^-)$	(7.I)	$\mu(H_2^+)+\mu(e^-)$	(7.II)
μ^{F}	$\mu(H_2^+)$	(8.I)	$\mu(H_2)$	(8.II)

(c). In order to find a relation between $\varepsilon^{\neq}$ and the reversible work required for the initial system to be brought from a standard state to a vacant site, ε^{I}, we introduce the Horiuti-Polanyi relation,[12]

$$\Delta\varepsilon^{\neq} = \alpha\Delta\varepsilon^{\mathrm{I}} = \alpha(\Delta\varepsilon + F\Delta\eta), \tag{9}$$

where α is a positive proper fraction. This equation is referred to step (I) or (II) where the initial system is $2H^+ + e^-$ or $H_2^+(a) + e^-$. $\Delta\varepsilon$ in the third term of the equation represents the change in ε by experi-

5) A. N. Frumkin, *Advs. Electrochem. Electrochem. Engineering*, **1**, 65 (1961).
6) O. H. Müller, *Polarography*, **1**, 319 (1966).
7) F. R. Smith and H. Heintze, *Can. J. Chem.*, **48**, 203 (1970).
8) R. Tamamushi, This Bulletin, **26**, 56 (1953).
9) G. C. Barker, "Trans. Sym. Electrode Processes", ed. Yeager, Wiley, New York (1961), p. 325.
10) *e.g.*, J. Horiuti and T. Nakamura, *Advs. Catal.*, **17**, 1 (1967).
11) J. Horiuti, *J. Res. Inst. Catal., Hokkaido Univ.*, **1**, 8 (1949—51).
12) J. Horiuti and Polanyi, *Acta Physicochim., U.S.S.R.*, **2**, 505 (1935).

mental conditions such as the kind of electrode. $F\Delta\eta$ represents the change in free energy of metal electron by polarization. Overvoltage, η, is taken positive for a cathodic polarization. Integration of Eq. (9) gives for steps (I) and (II),

$$\varepsilon_1^{\neq} = \alpha_1(\varepsilon+F\eta) + K_1 \quad (10.\text{I})$$

$$\varepsilon_2^{\neq} = \alpha_2(\varepsilon+F\eta) + K_2, \quad (10.\text{II})$$

where the sufficies 1 and 2 refer to steps (I) and (II) respectively, and K_1 and K_2 are integral constants. (d). $\mu(H^+)$, $\mu(e^-)$, and $\mu(H_2)$ are given as follows in reference to a standard state of the normal hydrogen electrode;

$$\mu(H^+) = RT \ln a_{H^+} \quad (11)$$

$$\mu(e^-) = F(-E_e+\eta) \quad (12)$$

and

$$\mu(H_2) = RT \ln P_{H_2}, \quad (13)$$

where a_{H^+} is an activity of H^+, E_e an equilibrium potential, and P_{H_2} a hydrogen pressure. E_e is given by

$$E_e = (RT/2F) \ln \{a_{H^+}^2/P_{H_2}\}. \quad (14)$$

i_1 and i_2. The forward current density of step (I), i_{+1}, is obtained from Eqs. (3), (5), (7.I), (10.I), and (11)$\sim$(13) as

$$i_{+1} = k_1 F a_{H^+} P_{H_2}^{1/2}(1-\theta) \exp\{[-\alpha_1\varepsilon+(1-\alpha_1)F\eta]/RT\}, \quad (15)$$

where $k_1 \equiv (kT/h)N^{\neq} \exp(-K_1/RT)$. Similarly, the backward current density of step (I), i_{-1}, is obtained from Eqs. (4), (5), (8.I), (10.I), and (11)$\sim$(13) as

$$i_{-1} = k_1 F\theta \exp\{[(1-\alpha_1)\varepsilon-\alpha_1 F\eta]/RT\}. \quad (16)$$

The net current density of step (I), i_1, is then

$$i_1 = k_1 F[a_{H^+}P_{H_2}^{1/2}(1-\theta) \exp\{[-\alpha_1\varepsilon+(1-\alpha_1)F\eta]/RT\} - \theta \exp\{[(1-\alpha_1)\varepsilon-\alpha_1 F\eta]/RT\}]. \quad (17)$$

The net current density of step (II), i_2, is obtained from Eqs. (3), (4), (6), (7.II), (8.II), (10.II), and (11)$\sim$(13) as

$$i_2 = k_2 F[a_{H^+}^{-1}P_{H_2}^{1/2}\theta \exp\{(1-\alpha_2)(\varepsilon+F\eta)/RT\} - P_{H_2}(1-\theta) \exp\{-(\alpha_2\varepsilon+\alpha_2\eta)/RT\}], \quad (18)$$

where $k_2 \equiv (kT/h)N^{\neq} \exp(-K_2/RT)$.

Equation (1) is now subjected to calculation by introducing Eqs. (17) and (18) for i_1 and i_2.

Calculation

Equations (17) and (18) show that i_1 and i_2 are as follows at given a_{H^+}, P_{H_2}, and α's;

$$i_1 \text{ or } i_2 = f(\theta, \eta, \varepsilon, k_1 \text{ or } k_2),$$

where k_1 and k_2 are parameters. In solving i_1 and i_2 as a function of θ, we need a relation between θ, ε, and η.

ε for $H_2^+(a)$. The adsorption energy of H_2^+(a), ε, will be given approximately by[13]

$$\varepsilon = \varepsilon_{00} + FE_p + R_e\theta, \quad (19)$$

where ε_{00} is the adsorption energy in the absence of potential difference from that of solution and at $\theta=0$, the second term an electrostatic potential energy at the plane where H_2^+(a) is located, and the third term a repulsive interaction energy between H_2^+(a)'s. In the present work, the repulsive energy is expressed to be proportional to the concentration of surrounding neighbours, *i.e.*, to θ.[14] R_e is the repulsive interaction energy at $\theta=1$. As the intermediate is a charged one, E_p and θ are interrelated in principle by the Poisson equation.

The Poisson Equation. To find the relation between E_p and θ, we employ Horiuti's model[13] (Fig. 1). P represents the plane on which H_2^+(a)'s are located. No charge is present between P and electrode surface, C. Beyond P, a diffuse double layer is present. The distance between C and P is x_p, and the dielectric constant is denoted by D_p in C–P and D_B beyond P. These dielectric constants are assumed to be potential-independent.

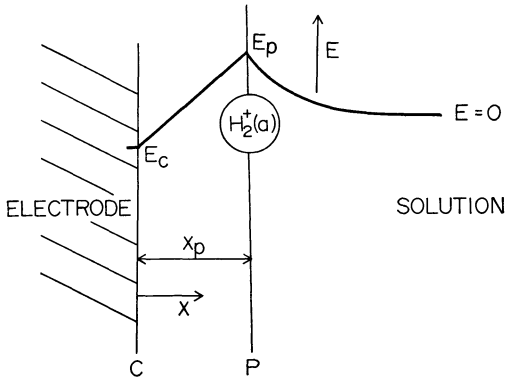

Fig. 1. A model for the double layer at interface.

Horiuti[13] analysed in detail the relation between E_p and θ as follows. One dimensional Poisson equation is given by

$$(D/4\pi)d^2E/dx^2 = -\rho, \quad (20)$$

where E is an electrostatic potential, and ρ is space charge density. Integration of Eq. (20) with respect to x gives at $x=x_p$,

$$-\frac{1}{4\pi}\lim_{t\to0}\left(D\frac{dE}{dx}\right)_{x_p-t} + \frac{1}{4\pi}\lim_{t\to0}\left(D\frac{dE}{dx}\right)_{x_p+t} = -\lim_{t\to0}\int_{x_p-t}^{x_p+t}\rho dx. \quad (21)$$

As there is no charge between C and P, the first term of the left hand side of Eq. (21) becomes $-D_p(E_p-E_c)/4\pi x_p$ where E_c is an electrostatic potential at C. The right hand side represents the charge on P, *i.e.*, $Q\theta$. Thus Eq. (21) becomes

$$-(D_p/4\pi x_p)(E_p-E_c) + (D_B/4\pi)\lim_{t\to0}(dE/dx)_{x_p+t} = -Q\theta. \quad (22)$$

The charge distribution beyond P is given for n mol/ml of 1–1 electrolyte solution by

$$\rho = Fn(e^{-FE/RT} - e^{FE/RT}). \quad (23)$$

13) J. Horiuti, *J. Res. Inst. Catal. Hokkaido Univ.*, **3**, 52 (1954).

14) The validity of proportional approximation is discussed by J. Horiuti and T. Toya, *Solid State Surface Science*, **1**, 1 (1969).

Since we have the relation $2d^2E/dx^2=d(dE/dx)^2/dE$, Eqs. (20) and (23) give

$$\lim_{t\to 0}\left(\frac{dE}{dx}\right)_{x_p+t} = \pm\left[-\frac{8\pi}{D_B}Fn\int_{E_p}^{0}(e^{-FE/RT}-e^{FE/RT})dE\right]^{1/2} \quad (24)$$

where $E=0$ and $dE/dx=0$ at $x\to\infty$.

We obtain from Eqs. (22) and (24)

$$C_{dl}(E_p-E_c)-(2D_BRTn/\pi)^{1/2}\sinh(FE_p/2RT) = Q\theta, \quad (25)$$

where $C_{dl}\equiv D_p/4\pi x_p$. Since the potential in bulk solution is zero, positive sign in Eq. (24) is chosen. Equation (25) becomes identical with the equation derived by Breiter *et al.*[15] when $\theta=0$.

In order to relate potential E with a measurable quantity, we take E_c as an electrostatic potential difference from the potential of point of zero charge E_z, *i.e.*, a rational potential, and assume that the work function of the electrode is constant over all overvoltage region. Thus E_c is given by

$$E_c = -\eta - E_z + (RT/2F)\ln(a_{H^+}^2/P_{H_2}). \quad (26)$$

The last term is due to the present choice of a standard state at normal hydrogen electrode (NHE). Thus, Eqs. (19), (25), and (26) give a relation for ε as a function of θ and η.

Two conditions for η. We selected the two following conditions so as to bring a transient behavior which can be easily tested by experiments.

(A) Constant Polarization: Variation of current i with time t was calculated at a constant polarization of the electrode to a certain η. The electrode can be initially in various conditions. In the present calculation, the initial condition of $\eta=0$ was chosen. Hence, θ at $t=0$ is an equilibrium value at $\eta=0$, $\theta_e°$. $\theta_e°$ was determined from Eqs. (1), (25), and (26) at $d\theta/dt=0$ and $\eta=0$. Since the polarization is a step function of t, E_p at $t=0$, $E_p°$ was determined from Eqs. (25) and (26) at $\eta=\eta$ and $\theta=\theta_e°$ (The Regula Falsi method was used).

(B) Potential Sweep: Current was calculated as a function of t (or η) when η was proportional to t. Initial condition was again chosen as $\eta=0$.

Calculations. The change of θ with t is given by Eq. (1) together with Eqs. (17) and (18). The relationship between θ and E_p is given by Eq. (25). The current at a certain time can be obtained from the solution of Eqs. (1) and (25). However, direct computation of these equations is so cumbersome that the derivative of Eq. (25) with respect to t is used for calculation; $d\theta/dt$ in the derivative is given by Eq. (1), $d\eta/dt$ being zero at condition (A) or equal to a sweep rate at condition (B). The Runge-Kutta-Gill method was used for calculations.

Parameters. Constants k_1 and k_2 are expected to have the relation $k_1\gg k_2$ since step (II) is slower than step (I). In the first calculation, k_2F was equated to the observed exchange current density, *i.e.*, $k_2=10^{-17}$ s^{-1} cm^{-2}. k_1 was chosen to be 10^5 times larger than k_2. We can evaluate ε_{00} by following the method of Horiuti *et al.*[13] However, the circumstances of the electrode seem to be more complicated than those treated by them, and hence $\varepsilon_{00}=-0.5$ eV was arbitrarily chosen. R_e was evaluated to be $26.7/D_p$ eV from coulombic repulsive force between H_2^+(a)'s on Hg whose atomic radius is 1.57 Å.[16] Each H_2^+(a) can be surrounded by six H_2^+(a)'s at full coverage. In the calculation, R_e was first taken to be 26.7 eV. The other parameters were, if not stated, $C_{dl}=18$ μF/cm², $E_z=-0.2$ V *vs.* NHE, $\alpha_1=\alpha_2=0.5$, and $a_{H^+}=P_{H_2}=1$.

Values of k_1, k_2, ε_{00}, R_e, C_{dl}, a_{H^+}, and E_z were further changed and their effects were examined.

The calculation was performed at Hokkaido University Computing Center with a FACOM 230—60 computer. Subroutine programs of Runge-Kutta-Gill and Regula Falsi methods furnished in FACOM were used.

Results

Condition (A). Figure 2 shows the relationship of logarithm of currents i_1, i_2, and i with time t at $\eta=0.2$ V. The relationships between log i and t are illustrated at various overvoltages in Fig. 3 where the result at $\eta=0.1$ V with $R_e=26.7/2$ eV is also shown. We see that the smaller R_e and overvoltage, the longer the time to attain a steady state. Coverage θ is plotted against t in Fig. 4. Comparison of Figs. 3 and 4 shows that the time to attain a steady value of θ is shorter than that of i at $\eta<0.3$ V. We denote steady values of i, θ, and E_p by i_s, θ_s, and E_{ps}, respectively.

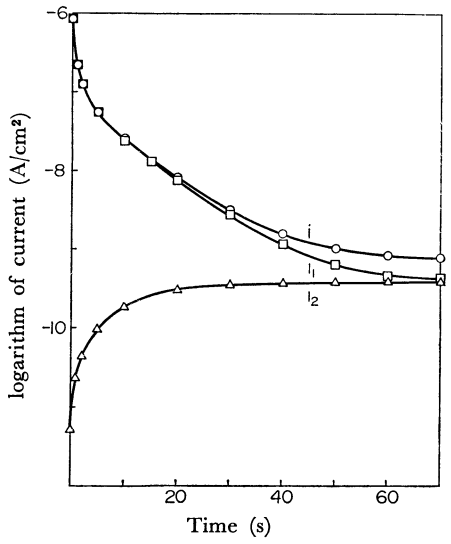

Fig. 2. Logarithm of currents i_1, i_2, and i *vs.* time curves at $\eta=0.2$ V (Condition (A)).

In Fig. 5, θ_s and E_{ps} in 1 M acidic solution are plotted as a function of η by the use of different set of values for the double layer capacity and the potential of the point of zero charge, *i.e.*, 18 μF/cm² and −0.2 V, 40 μF/cm² and −0.2 V, and 18 μF/cm² and −0.6 V (NHE), respectively. It is seen that θ_s first increases with η but becomes almost independent at

15) M. Breiter, M. Kleinerman, and P. Delahay, *J. Amer. Chem. Soc.*, **80**, 5111 (1958).

16) R. T. Sanderson, "Chemical Periodicity", Reinhold, New York (1964), p. 28.

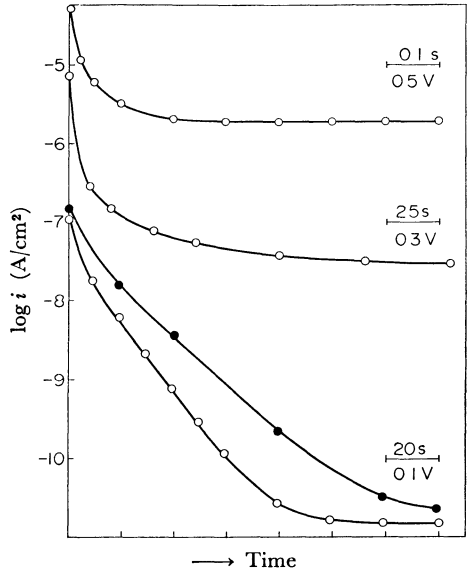

Fig. 3. $\log i$ *vs.* time curves at various overvoltages in Condition (A).
○, $R_e = 26.7$ eV; ●, 26.7/2 eV. Time scale is indicated for each curve. $k = 10^{-12}\,s^{-1}\,cm^{-2}$, $k_2 = 10^{-17}\,s^{-1}\,cm^{-2}$, $\varepsilon_{oo} = -0.5$ eV, $C_{dl} = 18\,\mu F/cm^2$, $E_z = -0.2$ V *vs.* NHE, and $a_{H^+} = P_{H_2} = 1$.

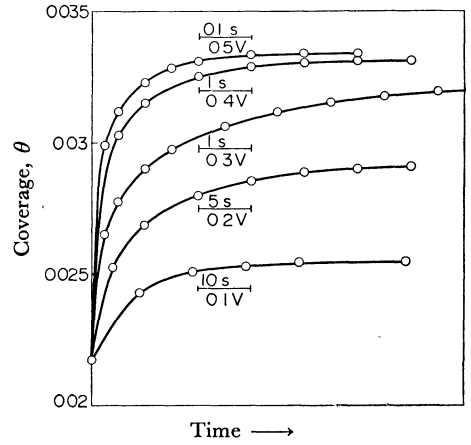

Fig. 4. Coverage *vs.* time curves at various overvoltages in Condition (A).
Time scale is indicated for each curve.

$\eta > 0.3$ V. E_{ps}, on the other hand, monotonously decreases with η. Tafel plots (the logarithm of i_s *vs.* η) for the above three sets of values give curve 2 in Fig. 6. Values of C_{dl} and E_z do not affect i_s to an appreciable extent at every overvoltage. We find that Tafel plots consist of two straight lines whose breakpoint coincides with that of the curve, θ_s *vs.* η in Fig. 5. The effect of the concentration of H^+ on the steady relation appears in the lower overvoltage region as shown by curves 1~3 in Fig. 6. The current density at a given overvoltage is larger for the smaller H^+ concentration. However, the dependence is reversed when η is replaed with the potential referred to NHE.

When only k_1 is decreased by an order of 10^2, the time to attain the steady state becomes considerably longer and θ_s becomes smaller than those in Figs. 3 and 5.

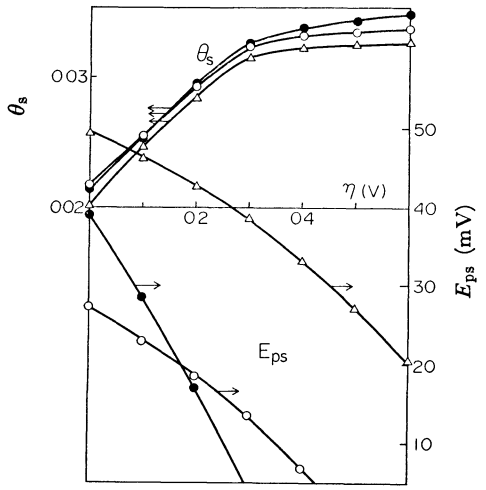

Fig. 5. θ_s and E_{ps} *vs.* η curves.
○, $C_{dl} = 18\,\mu F/cm^2$ and $E_z = -0.2$ V *vs.* NHE; ●, $C_{dl} = 40\,\mu F/cm^2$ and $E_z = -0.2$ V *vs.* NHE; △, $C_{dl} = 18\,\mu F/cm^2$ and $E_z = -0.6$ V *vs.* NHE.
E_{ps} is referred to the potential in the bulk of solution.

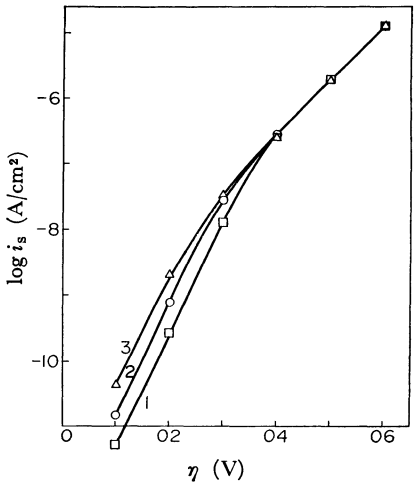

Fig. 6. Tafel plots at various H^+ concentration.
Curve 1(□), 10 N H^+; 2 (○), 1.0 N H^+; and 3 (△), 0.1 N H^+.

The variation of R_e causes a large change on $\log i$ *vs.* t (Fig. 3). On the other hand, our separate calculation shows that the change of ε_{00} does not appreciably affect $\log i$ *vs.* t and Tafel plots, except for θ and E_p. Thus, the changes of θ_s and E_{ps} are associated. The changes of double layer capacity and/or E_z affect θ_s and E_{ps} but neither $\log i$ *vs.* t nor Tafel plots.

Condition (B). With the same initial condition and parameters as in Fig. 3, a current was calculated up to $\eta = 0.5$ V for various sweep rates. The results are given in Fig. 7. It is interesting to see that the current plateau apprears on $\log i$ *vs.* η curve. The value of the current at the plateau is almost proportional to the sweep rate. In the overvoltage region lower than the plateau, $\log i$ *vs.* η represents the relationship of $\log i_1$ *vs.* η at $t \to 0$. In that higher than the plateau, the relation corresponds to Tafel plots ($\log i_s$ *vs.* η). The value of a current at the plateau i_p is computed for various values of parameters as in Condition (A)

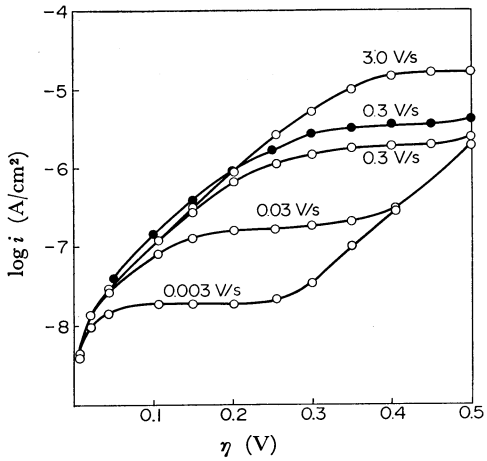

Fig. 7. log i *vs.* η curves at various potential-sweep rates in Condition (B).
○, $R_e=26.7$ eV; ●, $R_e=26.7/2$ eV.

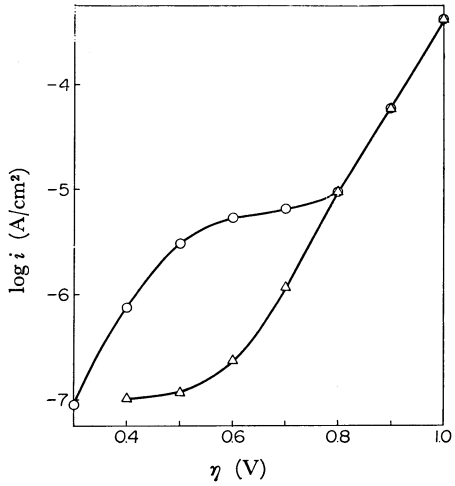

Fig. 8. log i *vs.* η curves in Condition (A).
$R_e=26.7/2$ eV, $k_1=10^{-14}$ s^{-1} cm^{-2}, and $k_2=10^{-19}$ s^{-1} cm^{-2} are used. ○, at a time of 90 ms after overvoltages are applied; △, at 5 s.

and found to be almost independent of them, except for R_e. i_p is nearly proportional to the reciprocal of R_e as seen from the curves for 0.3 V/s (solid and open circles in Fig. 7). The plateau has a tendency to lose its flat portion with increase of the sweep rate and to become shorter when the velocities of steps (I) and (II) become closer. Such a tendency makes it difficult to decide the value of i_p. In the case of $k_1/k_2=10^3$, i_s is one tenth smaller than that for $k_1/k_2=10^5$, where k_2 is kept at 10^{-17} s^{-1} cm^{-2} in both cases.

Discussion

In the above calculation, the value of k_2F was equated to the exchange current density determined by extrapolation of the linear part of Tafel plots at high overvoltages.[4] However, the calculated Tafel plots at high overvoltages show an appreciably larger current than the observed one. The discrepancy is due to the conventional linear extrapolation of Tafel plots observed at high overvoltages to $\eta=0$, whereas the present calculation reveals a break in the Tafel plots, giving the other linear portion with smaller Tafel slope at lower overvoltages. Such a break has been proposed by Horiuti *et al.*[17] When k_2 value is reduced to 10^{-19} s^{-1} cm^{-2} with $k_1/k_2=10^5$, Tafel plots reproduce the experimental data at high overvoltages. In this case, i_{+2} at $\eta=0$ becomes one hundredth of the extrapolated exchange current density.

Condition (A). The present calculation gives an interpretation for the depolarization at low overvoltages. The calculated log i *vs.* η at $t=5$ s and 90 ms is shown in Fig. 8, where $k_2=10^{-19}$ s^{-1} cm^{-2}, $k_1=10^{-14}$ s^{-1} cm^{-2}, and $R_e=26.7/2$ eV. The plots at $t=90$ ms show a typical S-type depolarization curve. Tza and Iofa,[18] and Iofa *et al.*[19] observed an S-type depolarization, which was markedly enhanced in the presence of specifically adsorbable anions. Former authors' interpretation, revised by Frumkin,[5] was based on the steady state treatment and successful only for the initial deviation from the linear part but not over all region. The present non-steady treatment has satisfactorily reproduced the whole S-type depolarization.

The depolarization contradicts Horiuti's prediction as commented by Frumkin.[5] Horiuti predicted that Tafel plots consist of the two linear parts with Tafel constants of 1.5 at low overvoltages and 0.5 at high overvoltages. The present work reproduces Horiuti's prediction in a steady state as seen in Fig. 6. Hence, the discrepancy will be due to a slow attainment of the steady state. The coverage in the steady state increases with the increase of overvoltage but becomes almost constant in the overvoltage region of Tafel constant of 0.5. It is interesting to see that θ itself is very small and approaches a limiting value by its increase in a very small amount; these results are attributed to the repulsive interaction between H_2^+(a)'s.

Coverage θ_e° is determined by the condition, $i_1=i_2=i=0$; Eqs. (17) and (18) show that ε_{00} and R_e are primarily important factors in a determination of θ_e°. ε_{00} is a parameter in the present calculation, and can not be estimated experimentally, although R_e is estimated from the experiments carried out with Condition (B). Tafel plots are also largely dependent on i_1 of step (I); the larger the α_1, the larger the Tafel slope.

At high overvoltages, Tafel plots at various H^+ concentrations give a single straight line. This is consistent with the observation, reviewed by Frumkin,[5] although he interpreted it on basis of the slow discharge mechanism. pH effect in a steady state can not manifest the principal mechanism.

Condition (B). The linear potential-sweep method has been employed for the study of dielectric relaxations, electrode processes, *etc.*

Let us suppose that adsorption process is expressed

17) J. Horiuti, A. Matsuda, M. Enyo, and H. Kita, "Proc. the 1st Australian Conference on Electrochem.", ed. Friend and Gutmann, Pergamon Press, Oxford (1965), p. 750.
18) Tza Chuan-sin and Z. A. Iofa, *Dokl. Akad. Nauk U.S.S.R.*, **126**, 1308 (1959).
19) S. Iofa, B. Kabanov, E. Kuchinski, and F. Chistyakov, *Acta Physicochim., U.S.S.R.*, **10**, 317 (1939).

by a series combination of the adsorption capacity c_{ads}, and the adsorption resistance r_{ads}. When the linear potential-sweep (sweep rate, v) is applied to such a circuit, the current of adsorption i_{ads} is given as $i_{ads}=v\ c_{ads}[1-\exp(-t/c_{ads}r_{ads})]$, where c_{ads} and r_{ads} are assumed to be constant. Hence, i_{ads} reaches finally a constant value of $v\ c_{ads}$. Appearance of the current plateau thus indicates the existence of adsorption process. If the pseudocapacity of H_2^+(a) c_p is given from a current plateau i_p and a sweep rate v by $i_p=v\ c_p$, we obtain 6 μF/cm^2 for $R_e=26.7$ eV and 12 μF/cm^2 for $R_e=26.7/2$ eV from Fig. 7. Such a simple calculation shows that c_p is strongly dependent on R_e.

However, r_{ads} in the present work is not constant as seen from the relation between i and η given by Eqs. (2), (17), and (18). This potential-dependent nature of r_{ads} is one reason for the shift of the current plateau to a more cathodic region with increase of the sweep rate. At lower overvoltages than the plateau region, log i *vs.* η is approximately equal to log i_1 *vs.* η so that we can estimate the velocity of the step preceding the rate-determining step. At higher overvoltages, log i *vs.* η represents its steady state, *i. e.*, Tafel plots, which agree with steady values calculated for Condition (A). Consequently, the potential-sweep method reveals information on the amount of pseudo-capacity, the velocity of the step preceding the rate-determining step, and the repulsive force energy constant of the proportional approximation.

Since a large value of the repulsive force between H_2^+(a)'s is expected from its Coulombic nature, the pseudo-capacity c_p may be quite small as calculated. The large value of R_e employed for the calculation, *i. e.*, 26.7 eV and 26.7/2 eV, does not necessarily mean that we insist on a value of D_p of unity or two. The present value of R_e is tentative and used only to give probable features.

In conclusion, potentiostatic and potentiodynamic transients have been calculated on the basis of the electrochemical mechanism of the hydrogen electrode reaction. The present double layer model and the repulsive force between adsorbates are somewhat simplified but the calculated results explain the depolarization observed at low overvoltages and give many predictions. Calculated features for the non-steady and steady states will be subjected to experimental tests and discussed in Part II.

The authors would like to express their appreciation to Professor T. Nakamura, Research Institute for Catalysis, Hokkaido University, for valuable discussion.